

The Measurement of Aerosol Optical Properties Using Continuous Wave Cavity Ring-Down Techniques

Anthony W. Strawa and Rene Castaneda

NASA Ames Research Center, Moffett Field, California

Thomas Owano, Douglas S. Baer^{*}, and Barbara A. Paldus

BlueLeaf Networks, Inc., Sunnyvale, California

* Current Affiliation: Los Gatos Research, Inc. Mountain View, California.

Corresponding Author address: Dr. Anthony W. Strawa, NASA – Ames Research Center, Mail Stop 245-4, Moffett Field, California.

The Measurement of Aerosol Optical Properties Using Continuous Wave Cavity Ring-Down Techniques

Anthony W. Strawa and Rene Castaneda

NASA Ames Research Center, Moffett Field, California

Thomas Owano, Douglas S. Baer^{*}, and Barbara A. Paldus

BlueLeaf Networks, Inc., Sunnyvale, California

Abstract

Large uncertainties in the effects that aerosols have on climate require improved in situ measurements of extinction coefficient and single-scattering albedo. This paper describes the use of continuous wave cavity ring-down (CW-CRD) technology to address this problem. The innovations in this instrument are the use of CW-CRD to measure aerosol extinction coefficient, the simultaneous measurement of scattering coefficient, and small size suitable for a wide range of aircraft applications. Our prototype instrument measures extinction and scattering coefficient at 690 nm and extinction coefficient at 1550 nm. The instrument itself is small (60 x 48 x 15 cm) and relatively insensitive to vibrations. The prototype instrument has been tested in our lab and used in the field. While improvements in performance are needed, the prototype has been shown to make accurate and sensitive measurements of extinction and scattering coefficients. Combining these two parameters, one can obtain the single-scattering albedo and absorption coefficient, both important aerosol properties. The use of two wavelengths also allows us to obtain a quantitative idea of the size of the aerosol through the Ångstrom exponent. Minimum sensitivity of the prototype instrument is $1.5 \times 10^{-6} \text{ m}^{-1}$ (1.5 Mm^{-1}). Validation of the measurement of extinction coefficient has been accomplished by comparing the measurement of calibration spheres with Mie calculations. This instrument and its successors have potential to help reduce uncertainty currently associated with aerosol optical properties and their spatial and temporal variation. Possible applications include studies of visibility, climate forcing by aerosol, and the validation of aerosol retrieval schemes from satellite data.

1. INTRODUCTION

The potential importance of aerosols in earth's climate has been well documented [Chylek and Coakley, 1974; Horvath, 1993], yet there remain significant uncertainties regarding their influence on the radiative balance in the atmosphere. The Intergovernmental Panel on Climate Change (IPCC) has identified radiative forcing due to aerosols as one of the most uncertain components of climate change models and as a topic urgently in need of further research [Houghton, 2001 #192]. Hansen *et al.* [1998] estimated the global-average direct forcing due to aerosols to be $-0.4 (\pm 0.3)$ W/m^2 and the indirect forcing due to aerosols through changes in cloud to be $-1.0 (+0.5/-1.0)$ W/m^2 . These large uncertainties are due to inadequate knowledge of aerosol optical properties and to their large spatial and temporal variation. Despite the importance of aerosol effects, little reduction of the uncertainties associated with these effects has occurred over the last ten years.

Regionally, radiative effects due to aerosols can be much larger than global effects [e.g., Kiehl and Briegleb, 1993, Russell et al., 1997]. Many studies [e.g., Hansen et al., 1998; Russell et al., 2002] have shown that accurate assessments of aerosol radiative effects require accurate values of aerosol single scattering albedo ω --the ratio of scattering to extinction. Recent experimental results have not provided the required accuracy. For example, in summarizing the results of the Clear Column Closure experiment conducted as part of the ACE 2 campaign, Russell and Heintzenberg [2000] stated that while measurements of ω generally agreed within the experimental accuracy of the individual instruments, this accuracy was not sufficient to adequately describe the effects of aerosols. More specifically, Russell et al. [2002] noted that in both TARFOX and ACE-2 different techniques yielded aerosol ω values differing by as much as 5% (0.90 to 0.95) when attempting to describe the same aerosol. They showed that, although the radiative effects of such large differences in ω could be very significant climatically (e.g., changing a cooling effect to a heating effect), it was not possible to determine whether the ω differences were experimentally significant because experimental uncertainties (typically 3% to 4% in those experiments) produced overlapping error bars.

In an important class of closure experiments remote measurements of aerosol extinction (scattering plus absorption) made with satellites and/or sunphotometers are compared with in situ measurements of size distribution, chemical composition, or optical properties. Measurements of chemical composition and absorption require long sampling times and often involve collection on filters or 'grab bags' for later analysis in the lab. These collection techniques cannot achieve the temporal and spatial resolution required for closure and they are usually attended with unacceptable artifacts. [Kirchstetter et al., 2001; Cui et al., 1998; Eatough et al., 1996] For example, Hartley et al. [2000] estimated uncertainties of as large as +/- 15% in ω deduced from in situ measurements made during TARFOX. What is needed is a direct way of measuring extinction or absorption in situ. Accurate values of aerosol extinction coefficient will also help validate satellite measurements and satellite retrievals of surface reflectance and atmospheric gas constituents.

The in situ measurement of extinction coefficient is particularly difficult because of the low levels of attenuation due to aerosol, on the order of 10^{-1} to 10^{-2} km^{-1} on the surface to 10^{-5} km^{-1} in the stratosphere.[Collins et al., 2000; Livingston et al., 2001] This is in contrast to the scattering coefficient, which is of the same magnitude as extinction but for which there are several in situ techniques, because in scattering, one measures the scattered light against a black background. With extinction, one measures a small decrease in a relatively bright light source. Since the shot noise of a measurement is related to the square root of the radiant power at the detector, the noise associated with the extinction measurement can be up to 1000 times greater than the scattering measurement of the same particulate. Currently in situ measurement of aerosol extinction requires very long path lengths and is primarily restricted to measurements of surface visibility. [Heintzenberg et al., 1997] The importance of the problem however has resulted in several attempts to measure extinction in situ on aircraft. One instrument designed to measure aerosol extinction on aircraft is the optical extinction cell (OEC) [Weiss and Hobbs, 1992] flown during the Smoke, Clouds, and Radiation-Brazil campaign (SCAR_B) in 1995. [Reid et al, 1998] This instrument measured the attenuation of light through a 6.4 meter tube and was used only for extremely high mass concentrations of aerosol, such as in smoke plumes. In an effort to achieve more sensitive measurements of aerosol extinction Gerber [1979a, 1979b] used a 2 m long white cell and a flow concentrator to achieve an effective optical path length of about 400 m. This instrument had a

measurement sensitivity of about 10^{-2} km^{-1} (10 Mm^{-1}) which is adequate for polluted surface environments but not at altitude or in cleaner environments at the surface.

This paper reports on the development of an instrument capable of sensitive and accurate in situ measurement of aerosol extinction and scattering coefficient using cavity ring-down (CRD) technology. We expect to be able to achieve an accuracy of 1% at 10 Mm^{-1} in extinction coefficient. The instrument is capable of fast ($< 30 \text{ sec.}$) sampling at two wavelengths from aircraft throughout the troposphere. Simultaneous measurement of the extinction and scattering signals will allow us to deduce the absorption coefficient and single-scattering albedo from our measurements. Briefly, CRD employs high reflectivity mirrors to achieve a path length of kilometers in a small cell. Since the technique was first demonstrated by O'Keefe and Deacon [1988] it has been used primarily for absorption spectroscopy. [O'Keefe et al., 1999] We expect that this instrument and its successors will help reduce uncertainty in optical properties and spatial and temporal variation of aerosols. Thus it will greatly contribute to visibility studies, aid in our understanding of climate forcing by aerosol, and assist in satellite validation and the validation of aerosol retrieval schemes from satellite data.

Section 2 of this paper briefly describes CRD, its application to the measurement of aerosol optical properties, and the design of the prototype instrument. In section 3 we consider the potential effects of this instrument on the uncertainty in measurements of aerosol optical properties. Initial measurements of laboratory-generated aerosol and instrument validation efforts are presented and discussed in section 4. Results from a field study and comparison with a nephelometer are also presented and discussed. Finally, future developments and improvements are outlined.

2. INSTRUMENT DESCRIPTION

An excellent review of the CRD techniques and applications can be found in the collection of papers edited by Busch and Busch [1999]. The principle behind CRD is briefly described here using the so-called 'ping-pong' model. A pulse of laser light is injected into a cavity that consists of two highly reflective mirrors. The mirror reflectivity is typically better than 99.96%. The laser pulse bounces between the two mirrors inside the ring-down cavity like a ping-pong ball. Each time

the pulse interacts with the back mirror, a small amount of light (e.g., 0.04%) leaks out. This light is collected and detected with a photomultiplier or similar detector. The intensity of the light leaking out of the back of the ring-down cavity decreases exponentially. It can be shown that the exponential decay, or ring-down time, is related to the mirror reflectivity and the absorption of the material inside the cavity by the relationship

$$\tau = \frac{L}{c} \left((1 - R) + \sigma_{ext} L + \sigma_{Ray} L + \sigma_{gas} L \right)^{-1} \quad (1)$$

where L is the cell length, c is the speed of light, R is the mirror reflectivity, σ_{ext} is the coefficient of extinction due to aerosol, σ_{Ray} coefficient of Rayleigh scattering, and σ_{gas} coefficient of absorption due to gaseous species in the cell. (Note that extinction is the sum of scattering plus absorption.)

While the ping-pong model explains the exponential decay of the signal, it is too simple to account for the fact that only light having frequencies near the cavity resonance mode will resonate in the ring-down cell. Thus, the laser linewidth must be mode-matched to a single cavity mode or multi-mode excitation in the cell will cause excessive noise. In this application a continuous wave (CW) laser source is used which results in several advantages over the pulsed laser technique. [Romanini et al., 1997] CW lasers diodes can be obtained with very narrow line widths that can be more effectively coupled into the cavity so that the sensitivity of the system is not limited by the laser linewidth. The resulting overlap between the laser and cell linewidth results in actual energy build up in the cell. This benefits both the extinction and the scattering measurements. CW laser diodes also have a higher duty cycle than pulsed lasers, which results in faster sampling. Finally, the use of CW laser diodes results in a more compact and rugged instrument suitable for aircraft operations. Pulsed laser systems are bulky and their sample rate is limited by the repetition rate of the laser, typically about 10 Hz.

In the present approach, extinction coefficient is given by the difference between measurements made when the cell contains filtered air and when the cell contains a particulate-laden flow:

$$\sigma_{ext} = \frac{1}{c} \left(\frac{1}{\tau_{aer}} - \frac{1}{\tau_0} \right) \quad (2)$$

where τ_{aer} is the ring-down time of the aerosol laden flow and τ_0 is for the filtered air. The minimum detectable absorption of CW-CRD systems is on the order of 10^{-4} to 10^{-6} km^{-1} . [Paldus and Zare, 1999] Thus a measurement accuracy in extinction coefficient of 1% to 0.01% is achievable at extinction levels of 10^{-2} km^{-1} .

Figure 1 shows the optical layout of the prototype system. It used two CW laser diodes at wavelengths of 690 nm and 1550 nm, located on the left. The laser beams are conditioned with spatial filters, combined with a dichroic beamsplitter, and coupled into a single cavity/flow cell. This instrument configuration consists of three mirrors that form a narrow isosceles triangle, unlike the two mirror system described in the ping pong model. One advantage of this configuration is that the light reflected from the input mirror will not couple back into the laser since the beam is reflected at 90° to the incoming beam. Input and output mirrors are set at 45 deg at one end of the cell and the third mirror is set at the other end of the cell 20 cm away. Light from the output mirror is focused onto the ring-down detectors that are located on the right of the diagram. One wall of the flow cell is made of BK-7 glass. In this configuration, the scattering detectors are located next to the glass wall. Aerosol-laden or filtered air enters the cell through 0.64 cm diameter tubing with a flow rate of 1.5 L/min. The optical path of the instrument, the path of the laser light through the aerosol-laden flow, was 36 cm. Figure 2 is a photograph of the instrument. The total size of the actual prototype instrument is small: 0.46 m x 0.61 m. The electronics associated with the instrument takes up half of an equipment rack, however, no attempt was made to minimize the size of the electronics for the prototype instrument. In this CW-CRD application, the back mirror is moved rapidly with a piezo-electric while monitoring the light output of the cell. When a resonance occurs, the light energy builds up in the cell and after it reaches a threshold, the laser is switched off rapidly, on the order of 50 ns. Ring-down times for this system are on the order of micro seconds. The ring down signal is then recorded as in pulsed-CRD. Ring-down occurs at a frequency of 50 to 100 Hz in this prototype system and 500 to 1000 shots were averaged over about 10 sec. to achieve one sample.

In order to obtain an accurate single-scattering albedo from a ratio of scattering to extinction coefficients, it is best to obtain measurements of both the scattering and extinction with the same instrument if possible. One reason for this is that it eliminates any variation that the aerosol optical properties may have as a function of wavelength. The second reason is that when the measurement is made within the same cell we are assured that the particle losses in the sample line, although they may be minimal, are identical and changes in relative humidity that may occur in the sample line are identical. With two different instruments this is not the case. Thus, our aim was to make the scattering coefficient measurement in the same cell as the extinction coefficient measurement.

One advantage of CW-CRD is that a buildup of energy occurs in the cell when the laser is in resonance with the cell. Resonance increases the output power of the cell and makes measuring the scattered signal easier. The light scattered by the aerosol will ‘ring-down’ exponentially once the laser is switched off. In our prototype, mirror reflectivity was not high enough to allow a measurement of the entire ring-down scattering signal. Only the scattering signal from the first several ring-down pulses was measured. This signal must of course be referenced to the laser power for every ring-down and can lead to more variation than is desired. In this system the scattering signal was calibrated by comparison with a Radiance Research Nephelometer and with the extinction signal for a non-absorbing aerosol.

It can be shown that the scattering coefficient is related to the ratio of scattering to ring-down signal and mirror reflectivity by the relation (see Appendix A)

$$\sigma_{sca} = \left(\frac{I_{sca}}{I_{rd}} \right) \frac{(1-R)}{(1+R)L} K \quad (3)$$

where I_{sca} and I_{rd} are the intensities of the scattered and ring-down signals, and K is a calibration constant. Thus, a more accurate measurement of the scattering coefficient can be obtained by taking the ratio of exponential fits to the scattering and ring-down signals. The ring-down time for both signals is the same. In this method, the scattering signal is automatically referenced to the laser power. Future versions of the instrument will have more highly reflecting mirrors so that the scheme presented in Equation (3) can be used to increase the scattering measurement sensitivity. Calibration gases will be used to calibrate the instrument as is standard in nephelometry. It is also possible to use non-absorbing spheres to calibrate the scattering signal.

Previous efforts to measure aerosol extinction with CRD are few. Sappey et al [1998] used a pulsed Nd-YAG laser source at 532 and 355 nm wavelength in a one meter cell to measure an extinction coefficient of $2 \times 10^{-7} \text{ m}^{-1}$ (0.2 Mm^{-1}). They compared the sensitivity of their system to that of a Met One Model 237H laser particle counter that uses light scattering to detect individual aerosol particles. Van der Wal and Ticich [1999] also used a pulsed system to measure soot volume fraction in flames. They were able to measure an extinction coefficient of $4 \times 10^{-1} \text{ km}^{-1}$ in a 1 cm sooting flame. More recently, Smith and Atkinson [2001] used a pulsed CRD system with a Nd-YAG laser to measure aerosol extinction at wavelengths of 532 and 1064 nm in a one meter cell. This system was similar to that of Sappey et al. and recorded an extinction of about $50 \times 10^{-6} \text{ m}^{-1}$ at a wavelength of 532 nm. A similar system is under development at the Desert Research Institute, Reno, NV. [Moosmuller, private communication]

Our system differs from these because it is a CW system and it is designed to operate on an aircraft simultaneously measuring the extinction and scattering coefficients. Instrument size, ruggedness, and sensitivity are of much more concern in an airborne application since space and weight are limited and the instrument is subjected to vibrations and temperature fluctuations. Also the extinction signal decreases with altitude. The wavelengths used in this system were selected to meet two criteria. They had to be obtainable with high quality laser diodes for size and repetition rate. The wavelengths were also selected to be near wavelengths used in other systems such as sunphotometers and satellites such as MODIS and Stratospheric Aerosol and Gas Experiment (SAGE) III.

3. CONSIDERATIONS OF MEASUREMENT UNCERTAINTY

The minimum detectable extinction of CW-CRD systems is on the order of 10^{-4} to 10^{-6} km^{-1} . [Paldus and Zare, 1999] Thus a measurement accuracy of from 1% to 0.01% is achievable at levels of extinction coefficient of 10^{-2} km^{-1} and we will be able to achieve the desired accuracy of 1% at 10 Mm^{-1} in extinction coefficient. While the extinction coefficient measurement itself does not need calibration, uncertainty will be introduced into the measurement by photon shot noise, digitization noise, particle losses and relative humidity changes within the instrument. The

scattering measurement will also be affected by non-idealities in the angular sensitivity of the instrument. These sources of error are very similar to those experienced by integrating nephelometers. Anderson et al. [1996] quote an uncertainty of 4-7% in measurements of scattering coefficient made with the TSI Model 3563 integrating nephelometer based on closure experiments with non-absorbing aerosols in the accumulation mode (0.1 to 1mm in diameter) in the laboratory. They state that this uncertainty is dominated by systematic uncertainties in non-idealities in wavelength and angular response which are a function of particle size. The intensity of light scattered from a particle is a function of the angle, θ , between the incident beam and the scattered light, the wavelength of the incident light, and particle size, shape and composition. One of the physical limitations of nephelometry is that any real diffuser cannot have a perfectly Lambertian profile (that is perfectly proportional to $\cos \theta$) and measure all angles from 0° to 180° . Larger particles scatter more light in the forward direction, near 0° . The best nephelometers have an angular response from 7° to 170° and this angular non-ideality is responsible for most of the uncertainty in the measurement. [Anderson et al., 1996] Additionally, uncertainties due to the dependence of the scattering on the wavelength of light will depend on the effective linewidth of the instrument. The CRD uses a laser of very narrow linewidth and this uncertainty is negligible. Nephelometers are calibrated with gases of known scattering coefficient. One advantage of our instrument is that we can also compare our measurements of extinction and scattering coefficients with lab-generated non-absorbing spheres to calibrate out effects due to angular non-idealities in the scattering measurement. Making the scattering and extinction measurements simultaneously will eliminate differences in the effects of particle loss and relative humidity changes within the instrument. The CRD instrument will not suffer from non-idealities in wavelength.

Here we compare uncertainties in the in-situ measurement of extinction and scattering coefficients and single-scattering albedo using several instrument combinations. To do this we will assume that uncertainties in the measurement of scattering coefficient with the integrating nephelometer and the CRD instrument are 7%, uncertainties in the measurement of extinction coefficient made with the CRD instrument are 1%, and uncertainties in the measurement of absorption coefficient made with an aethalometer are 30% as reported in Carrico et al. [2000] during the second Aerosol Characterization Experiment (ACE-2). It should also be noted that the aethalometer measurement is not as rapid as the other measurements, but this effect is ignored in this analysis.

Extinction coefficient is the sum of scattering and absorption coefficients. When the extinction coefficient is obtained by the sum of measurements of scattering and absorption coefficient its uncertainty is [Bevington and Robinson, 1992]

$$\delta_e^2 = \delta_s^2 + \delta_a^2, \quad (4)$$

where δ indicates the absolute uncertainty and the subscripts s, e, and a denote scattering, extinction and absorption, respectively. Since these are absolute uncertainties, the result is a function of the single-scattering albedo, ω . In terms of relative uncertainty this becomes

$$\left(\frac{\delta_e}{\sigma_{ext}}\right)^2 = \left(\omega \frac{\delta_s}{\sigma_{sca}}\right)^2 + \left(\frac{\bar{\omega}}{\omega} \frac{\delta_a}{\sigma_{abs}}\right)^2. \quad (5)$$

where the coalbedo is defined as $\bar{\omega} = 1 - \omega$. The uncertainties in the measurement of extinction coefficient measured with the CRD instrument are compared with the extinction coefficient obtained with a combination of nephelometer and aethalometer measurements in Figure 3a.

Uncertainties using the nephelometer and aethalometer measurements vary from 6.5 to 9% and the CRD measurement is a great improvement.

An independent measurement of the scattering coefficient can be obtained by taking the difference of the CRD extinction and aethalometer absorption measurements, taking advantage of the fact that the absorption is typically a small part of the total extinction to reduce uncertainty. When scattering coefficient is obtained as this difference, its uncertainty is

$$\delta_s^2 = \delta_e^2 + \delta_a^2. \quad (6)$$

In terms of relative uncertainty this becomes

$$\left(\frac{\delta_s}{\sigma_{sca}}\right)^2 = \left(\frac{\delta_e}{\omega \sigma_{ext}}\right)^2 + \left(\frac{\bar{\omega}}{\omega} \frac{\delta_a}{\sigma_{abs}}\right)^2. \quad (7)$$

The uncertainty derived from this relation is compared with the 7% uncertainty from the nephelometer in Figure 3b. It can be seen that for values of ω greater than 0.82, combining the measurements of the CRD and aethalometer give a better value for the scattering coefficient than the nephelometer.

Determining the uncertainty in ω is more complicated because the numerator and denominator are not independent. In general the relation to get the uncertainty in $\omega = \sigma_{sca}/\sigma_{ext}$ is [Bevington and Robinson, 1992]

$$\left(\frac{\delta_{\omega}}{\omega}\right)^2 = \left(\frac{\delta_e}{\sigma_{ext}}\right)^2 + \left(\frac{\delta_s}{\sigma_{sca}}\right)^2 - 2\frac{\delta_{se}^2}{\sigma_{sca}\sigma_{ext}}. \quad (8)$$

When the numerator and denominator are not independent measurements the covariance, δ_{se} , must be considered. For the case of combining a nephelometer measurement of scattering coefficient (with 7% uncertainty) with an aethalometer measurement of absorption coefficient (with an uncertainty of 30%), the fact that the same scattering measurement dominates in the numerator and denominator for large ω greatly reduces the uncertainty. A computer program has been written to evaluate equation 8 and the results are plotted in Figure 3c. The dominant source of uncertainty in the nephelometer scattering measurement are angular non-idealities, which do not occur in the CRD extinction measurement. Thus when combining a nephelometer or CRD measurement of scattering and CRD extinction measurements, the covariance term is not as effective at reducing uncertainty. When σ_{sca} is measured to 7% by the nephelometer and σ_{ext} is measured to 1% with the CRD, the uncertainty in ω is, surprisingly, independent of ω and about 7%. However, measurements of CRD extinction and aethalometer absorption coefficients can be combined to obtain the coalbedo, $\bar{\omega} = 1 - \omega = \frac{\sigma_{abs}}{\sigma_{ext}}$. In this case, with σ_{abs} measured to 30% by the aethalometer and σ_{ext} measured to 1% by the CRD, the uncertainty in ω becomes

$$\left(\frac{\delta_{\omega}}{\omega}\right)^2 = \left(\frac{\delta_{\bar{\omega}}}{\bar{\omega}}\right)^2 = \left(\frac{\bar{\omega}}{\omega} \frac{\delta_{\bar{\omega}}}{\bar{\omega}}\right)^2 \quad (9)$$

$$\frac{\delta_{\omega}}{\omega} = \frac{\bar{\omega}}{\omega} \left[\left(\frac{\delta_a}{\sigma_{abs}}\right)^2 + \left(\frac{\delta_e}{\sigma_{ext}}\right)^2 \right]^{1/2}. \quad (10)$$

The results are compared with the results of Equation 8 in Figure 3c. Using the CRD extinction, uncertainties in ω are comparable to those using nephelometer scattering and aethalometer absorption.

4. RESULTS

The performance of the prototype instrument was tested by generating various types of aerosols in our laboratory and measuring their optical properties. Figure 4 shows a plot of measured extinction coefficient versus particle number density for various particle compositions: ammonium sulfate, and polystyrene spheres (PSS) of 0.72 and 1.05 μm in diameter. Particle number density was measured with a TSI Model 3025 Condensation Particle Counter (CPC). Both laser wavelengths, 690 and 1550 nm, measured a minimum extinction coefficient of about $1.5 \times 10^{-6} \text{ m}^{-1}$ (1.5 Mm^{-1}) for ammonium sulfate aerosol. This is a significant improvement in performance over the Smith and Atkinson [2001] instrument, especially when the 20 cm cell length is compared to their 1 m length. Sappey et al. [1998] achieved a sensitivity of 0.2 Mm^{-1} in their 1 m cell. Our goal is to improve upon this performance in an instrument that is small enough to fly on any aircraft. Planned improvements in the instrument are outlined in Section 4. The sensitivity of the flight instrument is expected to be at least an order of magnitude better than the performance of the prototype. The dynamic range of the prototype instrument is seen to be about 3.5 orders of magnitude.

One of the advantages of the CRD technique is that it provides an absolute measurement of the extinction coefficient, meaning that it needs no calibration. Nevertheless, it is important to verify the performance of any new instrument. This is a difficult task because no independent measure of aerosol extinction coefficient at typical atmospheric conditions is available in a laboratory setting. Thus we attempted to verify the performance of the prototype instrument by comparing the measurement of extinction coefficient of calibration PSS with calculations using a Mie code [Wiscombe, 1980]. Figure 5 shows this comparison for 1.05 μm PSS and both laser wavelengths. The index of refraction used for PSS was (1.45, 0.0) and the number density was obtained from CPC measurements. Vertical bars indicate the standard deviation in the extinction measurement and horizontal bars represent the standard deviation in the number density measurement. Much of this variability was due to variations in the aerosol number density produced by the aerosol generator used. The variation in the number density does not affect instrument performance since the measurement of extinction coefficient is not dependent on a measure of the number density. It does, however, complicate verification. Another factor affecting variability in the signal for low number densities is the size of the sample volume. Assuming that the effective beam diameter in the cell is 2 mm, the effective sampling volume of the instrument is about 0.6 cm^3 . In our experiments with ammonium sulfate aerosol, a sensitivity of 1.5 Mm^{-1} was achieved for a number density of about 20

cm^{-3} . This means that about 12 particles were in the sample volume at any one time. As the number density of the sampled aerosol increases, the variability in the signal due to the number of scatterers in the sample volume should decrease, a trend seen in Figure 5. Number densities decrease as extinction coefficient decreases and the statistics of whether or not a particle is in the sample volume could represent a significant portion of the variability in the signal. Some strategies that avoid this problem are increasing the cell optical path and increasing the averaging time.

One reason for discrepancies between the calculation and measurement is the presence of other scatterers in the sample stream besides the calibration spheres. Figure 6 shows a typical size distribution obtained with a Particle Measurement Systems Passive Cavity Aerosol Spectrometer Probe (PCASP) for the aerosol produced by our aerosol generator. PSS of $1.05 \mu\text{m}$ in diameter were mixed in de-ionized, filtered water, and an aerosol was produced by atomization with dry filtered air. The aerosol was subsequently dried to a relative humidity of less than 10 %. Note that the peak at about $1.05 \mu\text{m}$ is very broad and that there is a significant distribution of aerosol due to impurities in the water. This contamination is omnipresent with this type of aerosol generation. An attempt was made to estimate what portion of the aerosol that entered the prototype instrument was optically active and this number was used in the Mie calculation. Until we generate a monodisperse aerosol with very little variation in number density we cannot truly assess the accuracy of this instrument. In order to improve the agreement between the measured extinction and that deduced from size distributions of calibration spheres, much more attention needs to go into the generation of the aerosol and characterization of its physical properties, i.e., number density and size. In future laboratory experiments, the use of a more constant output aerosol generator and an electrostatic classifier will eliminate much of the uncertainty in the calculated extinction coefficients by producing a more constant, monodisperse aerosol for instrument validation. An electrostatic classifier can select out aerosol within a very narrow size range for analysis with our instrumentation.

One advantage of a measurement at multiple wavelengths is that a qualitative idea of the optically effective particle size can be obtained by calculating the Ångström exponent, Å . Generally, Å decreases as the particles become larger. Ångström exponents were calculated from the measurements shown in Figure 4 for number densities greater than 80 cm^{-3} yielding $\text{Å} = -0.15$ for

1.05 mm diameter PSS, $\lambda = 0.15$ for 0.72 mm diameter PSS, and $\lambda = 0.26$ for ammonium sulfate particles. Calculated values are $\lambda = 0.14$ for 1.05 mm diameter PSS, $\lambda = 0.65$ for 0.72 mm diameter PSS. The difference between the λ calculated and deduced from measurements probably reflects the polydisperse nature of the size distribution. PCASP size distributions of the ammonium sulfate aerosol showed that the distribution peaked at about 200 nm, in agreement with the λ obtained from the measurements.

After the initial laboratory tests were completed, the instrument was involved in some limited field work at NASA-ARC. Air was drawn through a common stack approximately 3 meters from the instruments, with an inlet 20 meters above the ground, and sampled by the prototype instrument, a Radiance Research nephelometer, CPC, and PCASP. Figure 7 shows results from a portion of this test. Extinction coefficients at 690 and 1550 nm measured with the prototype are plotted in Figure 7a; scattering coefficient from the prototype instrument and the nephelometer are plotted in Figure 7b; and volume density measured by the PCASP is plotted in Figure 7c. Scattering at 1550 nm was not obtained in this instrument configuration. At approximately 35 min into the test, flow to the prototype instrument and nephelometer was switched to filtered air for 5 min to obtain a zero for the extinction measurement. The aerosol-laden flow to the PCASP was not interrupted. During this sampling period the airfield fire department conducted a practice exercise, lighting a small petroleum fire and extinguishing it with water. This generated a white plume that dissipated and passed over our location at approximately 50 min. The signature of the plume can be seen in all of the instruments.

Agreement between the scattering coefficient measured with the prototype instrument and the nephelometer is good in the first 50 minutes of the field test although the prototype instrument shows more variability than the nephelometer. This is due in part to actual variability in the aerosol that the slower response nephelometer did not capture and evidence of this variability can also be seen in the extinction measurement. During the plume event, however, the scattering coefficient measured by the nephelometer is larger than that measured by the prototype. The angular response of the prototype was approximately from 15° to 165° from the forward scatter direction. This angular response is not adequate to completely measure the forward scattering signal from the large scatterers that were present during the plume event and would result in a smaller scattering signal

as observed. The fact that the prototype signal drops off earlier than the nephelometer signal is due to response time. By improving the angular response of the scattering detector and by measuring the entire scattering signal as outlined in Section 2, we expect that the accuracy and sensitivity of the scattering measurement will improve with the next generation instrument.

The Ångstrom exponent calculated from the measurement before the plume arrived was about 1.23 while during the plume α was 0.88 indicating growth in the particles during the plume event. This is borne out in a comparison of PCASP size distributions taken at 3 and 55 min and shown in Figure 8. The hypothesis is that the fire produced carbonaceous, absorbing material. Water vapor produced from the water used to extinguish the fire, condensed onto the combustion and ambient aerosol as the air cooled. As a result, one would expect an increase in the number density, the size of the particles, and in ω of the particles as water condensed onto the aerosol. These trends are borne out in the data. Also note the suggestion of an increase in the coarse particle mode (greater than 2 microns) in Figure 8 at 55 min.

Finally we deduce ω and absorption coefficient from the prototype measurements. The ω prior to the plume event was about 0.8 using the prototype scattering coefficient and 0.75 using the nephelometer scattering coefficient. The difference between these values of about 5% represents the inaccuracies in the prototype scattering measurement as discussed above. The objective of the prototype design was to demonstrate the feasibility of the measurement scheme and instrument improvements outlined in Section 4 will greatly improve instrument accuracies. These values of ω seem to be low for the type of environment at our location. The prototype measurement is more variable reflecting the higher degree of variability in the scattering signal and quite likely variability in the actual aerosol. During the plume event ω increases as one would expect as a large number of more highly reflecting particles is encountered. The ω obtained during the plume event using the prototype scattering coefficient is about 1.0, while the ω obtained with the nephelometer is slightly greater than 1.0. Absorption coefficients deduced from the measurements yield 7 Mm^{-1} before the plume and 10 Mm^{-1} during the plume. The increase in absorbing material accompanied with an increase in the ω during the plume event is consistent with the hypothesis that the fire produced absorbing material and that water used to extinguish the flames condensed onto the aerosol.

4. CONCLUSIONS

This paper describes the development, validation, and employment of an instrument designed to measure aerosol extinction and scattering coefficients using CW-CRD. The instrument is unique since it is the first application to the measurement of aerosol optical properties using CW-CRD, it is designed for the simultaneous measurement of extinction and scattering at two wavelengths, and its small size and ruggedness make it suitable for application on airborne platforms. The prototype instrument has been built and tested in our lab and used in the field. The prototype has successfully made measurements of extinction and scattering coefficients. Improvements in the measurement of both of these quantities are indicated, however, modifications can easily be made which will greatly improve the accuracy and sensitivity of both of these quantities. Combining these two quantities, one can obtain the single-scattering albedo and absorption coefficient, both important aerosol properties. The use of two wavelengths also allows us to obtain a quantitative idea of the size of the aerosol through the Ångström exponent.

Minimum sensitivity of the prototype instrument is $1.5 \times 10^{-6} \text{ m}^{-1}$ (1.5 Mm^{-1}). Validation of the measurement of extinction coefficient has been accomplished by comparing the measurement of calibration PSS by the prototype instrument with Mie calculations. This method yielded satisfactory results, however, improvements in both the instrument and in the calibration technique have been identified and are discussed below. In order to truly assess the accuracy of this instrument, we must improve our ability to generate a stable stream of monodisperse calibration aerosols. The equipment needed to accomplish this has been identified. The prototype instrument has been successfully used in the field. Measurements of scattering coefficient are compared with a state-of-the-art nephelometer and agreement is good. Absorption coefficient and single-scattering albedo deduced from the prototype measurements are reasonable considering the state of the ambient aerosol before and during sampling of a fire plume. Further lab and field tests are planned.

The next generation instrument should have several improvements. Instrument sensitivity and particle loss inside the instrument need to be better characterized. Most importantly, the mirrors need to be kept as clean as possible. Decreases in mirror reflectivity contributed greatly to

uncertainties in initial measurements with the prototype system. All of these factors are being currently addressed. The sensitivity of the measurement of extinction and scattering coefficient can be improved by the use of more highly reflective mirrors. This helps by increasing the ring-down time which allows for a more precise and sensitive extinction measurement. The resulting build up of radiant energy in the cell also improves the scattering measurement. An improved flow design will be employed to help keep the mirror surfaces clean and to avoid putting the particle-laden flow through small tubes and tight turns. A better optical scheme for the scattering measurement will be used. It is expected that this instrument will be capable of making particulate extinction and scattering measurements from the surface to the upper-troposphere to an accuracy of 1% for extinction coefficients of 10^{-3} km^{-1} (0.1 Mm^{-1}). Improved electronics will result in increased repetition rates on the order of 500 to 2000 Hz. This improvement can decrease the acquisition time or allow averaging over more samples for greater sensitivity. An instrument with this capability could will reduce uncertainty currently associated with aerosol optical properties and their spatial and temporal variation. It could contribute to visibility studies, aid in our understanding of climate forcing by aerosol, and assist in satellite validation and the validation of aerosol retrieval schemes from satellite data.

Acknowledgements

The authors wish to thank Mr. Uwe Horchner for developing the instrument software and Mr. Eric C. Crosson for many useful discussions relating to instrument design. This work has been supported by NASA's Small Business Innovative Research and Upper Atmosphere Research Programs. The authors also wish to thank the reviewers for many helpful comments.

REFERENCES

- Anderson, T. L. and e. al. (1996). "Performance characteristics of a high-sensitivity, three-wavelength, total scatter/backscatter nephelometer." J. Atmos. and Oceanic Tech. **13**(5): 967.
- Bevington, P. R. and D. K. Robinson (1992). Data reduction and error analysis for the physical sciences. Boston, WCB McGraw-Hill.
- Busch K.W. and M.A. Busch, (1999). "Cavity Ringdown Spectroscopy, American Chemical Society, Washington, D.C.
- Carrico, C. M., M. J. Rood, et al. (2000). "Aerosol Optical properties at Sagre, Portugal during ACE-2." Telus **52B**(2): 694-715.
- Chylek and Coakley (1974). "Aerosols and Climate," *Science*, 183, 75-77.
- Collins, D. R., Jonsson, H. H., Seinfeld, J. H., Flagan, R. C., Gassó, S., Hegg, D., Russell, P. B., Livingston, J. M., Schmid, B., Öström, E., Noone, K. J., and Russell, L. M. 2000. In situ aerosol size distributions and clear column radiative closure during ACE-2. *Tellus 52B*, 498-525, 2000.
- Cui, W., D.J. Eatough, and N.L. Eatough, (1998). "Fine particulate organic material in the Los Angeles Basin," *J. of Air and Waste Management Assn.* 48, 1024-1037.
- Eatough, D.J., D.A. Eatough, L.Lewis, E.A. Lewis, (1996). Fine particulate chemical composition and light extinction at Canyonlands National Park using organic particulate material concentrations obtained with a multi-system, multi-channel diffusion denuder sampler," *J.Geophys. Res.* 101, 19515-19531.
- Gerber, H. E. (1979). "Absorption of 632.8 nm radiation by maritime aerosols near Europe." *J. Atmos. Sci.* 36: 2502-2512.
- Gerber, H. E. (1979). "Portable cell for simultaneously measuring the coefficients of light scattering and extinction for ambient aerosols." *Applied Optics* 18(7): 1009-1014.
- Gerber, H., C. H. Twohy, et al. (1998). "Measurements of wave-cloud microphysical properties with two new aircraft probes." *Geophys. Res. Lett.* 25(8): 117-1120.
- Hartey, W.S., P.V. Hobbs, J.L. Ross, P.B. Russell, and J.M. Livingston, (2000). "Properties of aerosols aloft relevant to direct radiative forcing off the mid-Atlantic coast of the United States," *J. Geophys. REs.*, 105, 9859-9885.

- Hansen *et al.* "Climate forcing in the industrial era." PNAS 95, 12753 (1998).
- Heintzenberg, J., R.J. Charlson, A.D. Clarke, C. Liousse, V. Ramaswamy, K.P. Shine, M. Wendisch, and G. Helas. (1997). "Measurements and modeling of aerosol single-scattering albedo: progress, problems, and prospects," *Beitr. Phy. Atmosph.* 70, 249-263.
- Houghton, J. T., Y. Ding, et al. (2001). *Climate change 2001: The Scientific Basis*. Cambridge, Cambridge University Press.
- Horvath, H. (1993). "Atmospheric Light Absorption – A review," *Atmos. Environ.* 27A, 3, 293-317.
- Kiehl, J. T., and B. P. Briegleb, The relative roles of sulfate aerosols and greenhouse gases in climate forcing, *Science*, 260, 311-314, 1993.
- Livingston, J M, P B Russell, B Schmid, J Redemann, J A Eilers, S A Ramirez, R Kahn, D Hegg, P Pilewskie, T Anderson, S Masonis, T Murayama, ACE-Asia Aerosol Optical Depth and Water Vapor Measured by Airborne Sunphotometers and Related to Other Measurements and Calculations, *EOS Trans. AGU*, 82(47), Fall Meet. Suppl., Abstract A22A-0094, 2001.
- Romanini, D., Kachanov AA, Sadeghi N, and Stoeckel F. (1997). "CW cavity ring down spectroscopy," *Chem. Phys. Lett.*, 264 , 3-4, 316-322.
- O’Keefe A. and D.A.G. Deacon, "Cavity ring-down optical spectrometer for absorption measurements using pulsed laser sources," *Rev. Sci. Inst.*, 59(12):2544 (1988).
- O’Keefe, A, J.J. Scherer, J.B. Paul, and R.J. Saykally (1999). "Cavity Ringdown Laser Spectroscopy: History, Development, and Applications," in *Cavity-Ringdown Spectroscopy*, eds. Busch and Busch, American Chemical Society, Washington, D.C.
- Pladus, B.A. and R.N. Zare (1999). "Absorption Spectroscopies: From early beginnings to cavity-ringdown spectroscopy," in *Cavity-Ringdown Spectroscopy*, eds. Busch and Busch, American Chemical Society, Washington, D.C.
- Reid, J.S., P.V. Hobbs, C. Liousse, J. Vanderlei Martins, R.E. Weiss, and T.F. Eck, (1998). "Comparisons of techniques for measuring shortwave absorption and black carbon content of aerosols from biomass burning in Brazil," *J. Geophys. Res.*, 32,031-32,040.
- Russell, P. B., S. Kinne, and R. Bergstrom, Aerosol climate effects: Local radiative forcing and column closure experiments, *J. Geophys. Res.* 102, 9397-9407, 1997.
- Russell, P. B., J. Redemann, B. Schmid, R. W. Bergstrom, J. M. Livingston, D. M. McIntosh, S. Hartley, P. V. Hobbs, P. K. Quinn, C. M. Carrico, M. J. Rood, E. Öström, K. J. Noone, W. von

- Hoyningen-Huene, and L. Remer, Comparison of aerosol single scattering albedos derived by diverse techniques in two North Atlantic experiments, *J. Atmos. Sci.*, 59, 609-619, 2002.
- Russell, P. B. and J. Heintzenberg (2000). "An overview of the ACE-2 clear sky column closure experiment (CLEARCOLUMN)." *Tellus* 52(2): 463-483.
- Sappey, A. D., E. S. Hill, et al. (1998). "Fixed-frequency cavity ringdown diagnostic for atmospheric particulate matter." *Optics Letters* 23(12): 954-956.
- Smith, J.D., and D.B. Atkinson. (2001). "A portable pulsed cavity ring-down transmissometer for measurement of the optical extinction of the atmospheric aerosol," *Analyst*, 126, 1216-1220.
- Vander Wal, R. L. and T. M. Ticich (1999). "Cavity ringdown and laser-induced incandescence measurements of soot." *Applied Optics* 38(9): 1444-1451.
- Weiss, R.E. and P.V. Hobbs (1992). "Optical extinction properties of smoke from the Kuwait oil fires," *J. Geophys. Res.*, 97, 14,537-14,540.
- Wiscombe, W., 1980. "Improved Mie Scattering Algorithms." *Applied Optics*, 19, 1505-1509.

Appendix A. Derivation of Equation 3.

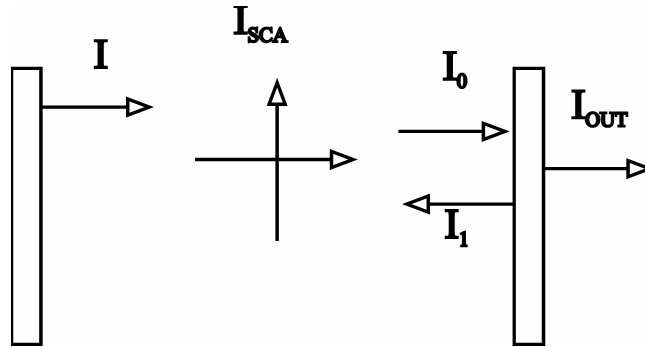


Figure. A1. Schematic of ring-down cell showing scattering.

Consider an ideal CRD cell of length, L , and mirror reflectivity, R , filled with an aerosol. Incident light enters through the front mirror with an intensity I . The light bounces back and forth between the front and back mirrors. During each round trip some of the light is transmitted through the back mirror and some is reflected back in the cell. Let I_0 be a light pulse interacting with the back mirror. I_{OUT} is the light transmitted through the back mirror and is the ring-down signal and I_1 is the light reflected by the back mirror. I_{SCA} is the light scattered as I_1 interacts with particles in the cell and σ_{SCA} is the scattering coefficient. The following relationships hold:

$$I_{OUT} = I_0(1 - R), \quad \text{A1}$$

$$I_1 = I_0 R. \quad \text{A2}$$

$$\text{Thus, } I_1 = I_{OUT} \frac{R}{(1 - R)}. \quad \text{A3}$$

Note that the finesse of the cell is

$$\pi \sqrt{R} / (1 - R). \quad \text{A4}$$

The light scattered from the cell on this round trip can be written as

$$I_{SCA} = I_0 \sigma_{sca} L + I_1 \sigma_{sca} L. \quad \text{A5}$$

Combining equations A3 and A5 we have

$$I_{SCA} = I_{OUT} \sigma_{sca} L (1 + R) / (1 - R), \quad \text{A6}$$

$$\text{or } \sigma_{sca} = \frac{I_{SCA}}{I_{OUT}} \frac{(1 - R)}{(1 + R)L}. \quad \text{A7}$$

Thus the scattered light is proportional to the ring-down signal and the ring-down times for both signals are the same. The scattering coefficient can be most accurately obtained by taking the ratio of an exponential fit of the scattering signal to an exponential fit of the ring-down signal. A real detector, of course, will see only a small portion of I_{SCA} and the instrument must be calibrated to obtain the scattering coefficient. The relationship A7, however, allows the use of many more points in the fit thus increasing accuracy.

Figures

Figure 1. Schematic of prototype instrument

Figure 2. Photo of prototype instrument

Figure 3. Comparison of Uncertainty for extinction and scattering coefficient and single-scattering albedo for various combinations of measurements. (a) Comparison of uncertainty in CRD extinction coefficient measurement with that deduced from a combination of nephelometer and aethalometer measurements. (b) Comparison of uncertainty in nephelometer scattering measurement with that deduced from a combination of CRD and aethalometer measurements. (c) Comparison of uncertainty in single-scattering albedo from the combination of using CRD extinction with CRD nephelometer scattering and aethalometer absorption with the combination of nephelometer scattering and aethalometer absorption.

Figure 4. Measurements of extinction coefficient versus number density for various aerosol composition and size. a) wavelength = 690 nm, b) wavelength = 1550 nm

Figure 5. Measurements of extinction coefficient versus number density for 1.05 μm diameter polystyrene calibration spheres compared with Mie calculations. a) wavelength = 690 nm, b) wavelength = 1550 nm.

Figure 6. PCASP size distribution of 1.05 μm PSS with water.

Figure 7. Field measurement. a) Extinction coefficient at both wavelengths; b) Prototype scattering measurement compared with Radiance Research nephelometer; c) volume density versus time from PCASP. The dip in signal in a and b at 35 minutes results from zero air. The peak at 50 minutes results from a plume encounter.

Figure 8. Size distributions from PCASP for two time periods, 3 and 55 minutes.

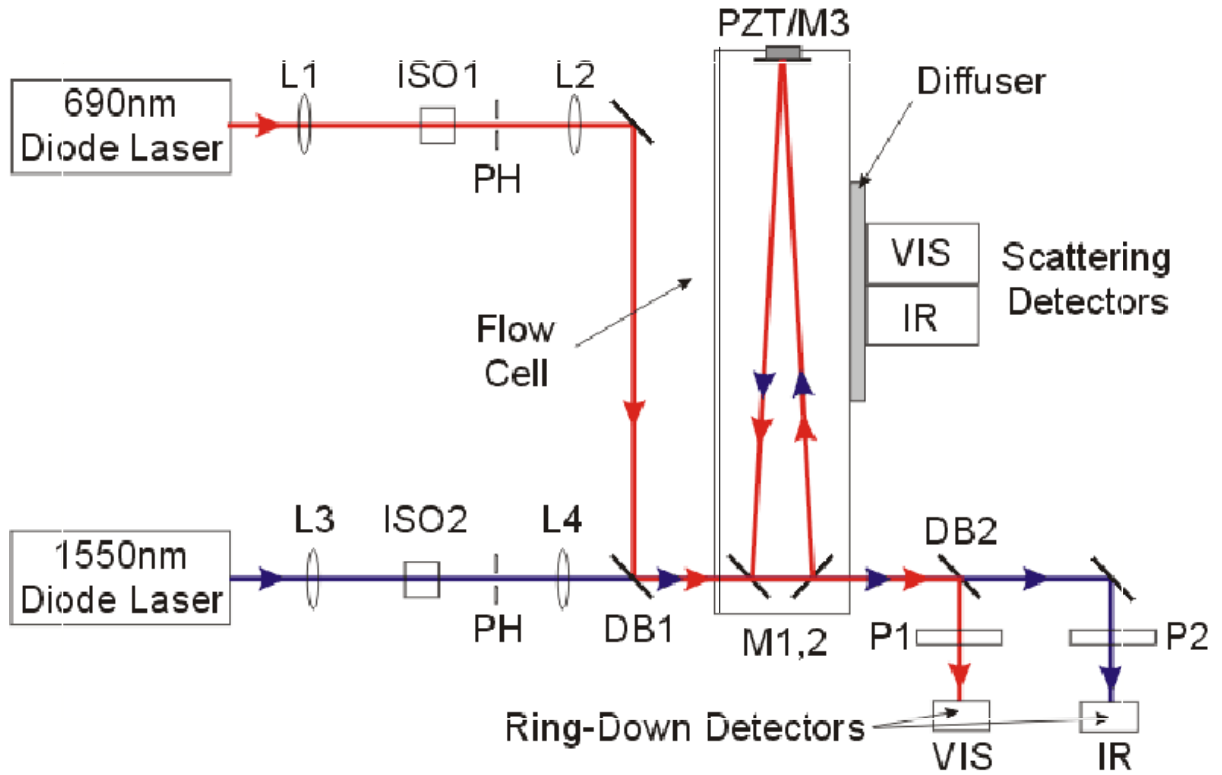


Figure 1. Schematic of prototype instrument.

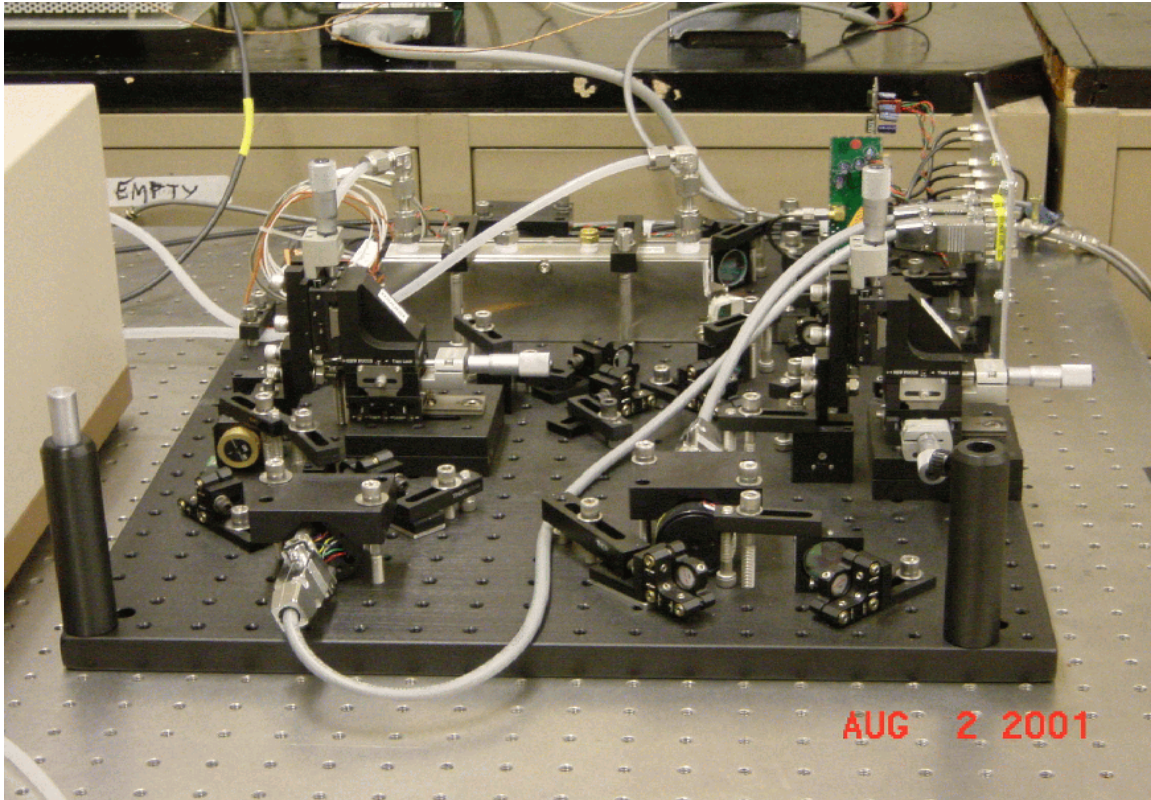
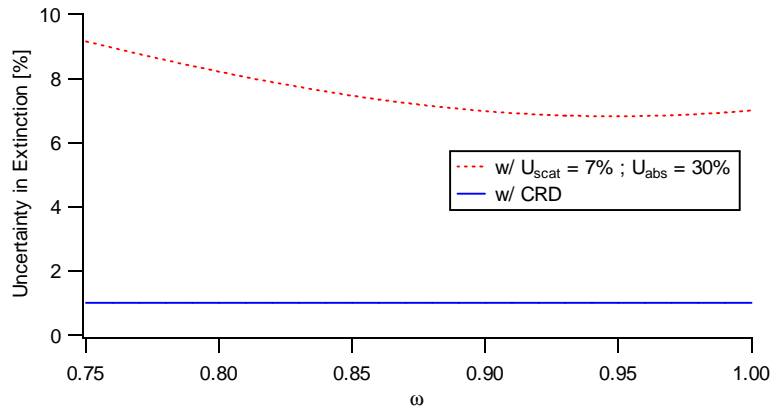
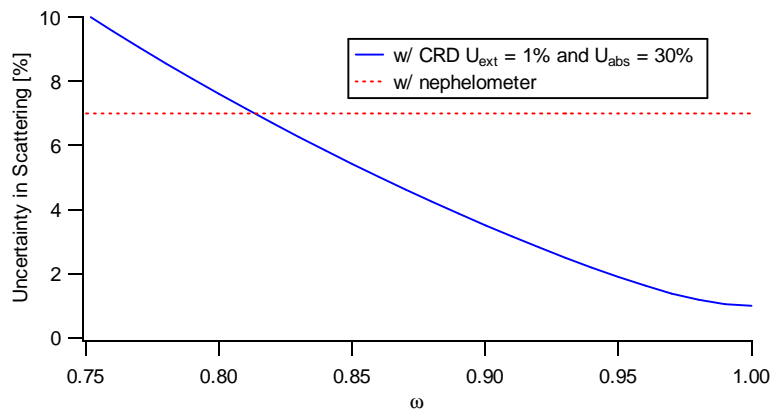


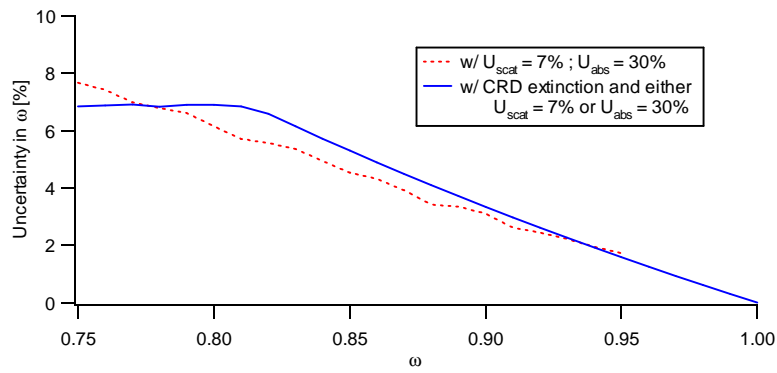
Figure 2. Photo of prototype instrument in Lab at NASA-ARC.



(a)

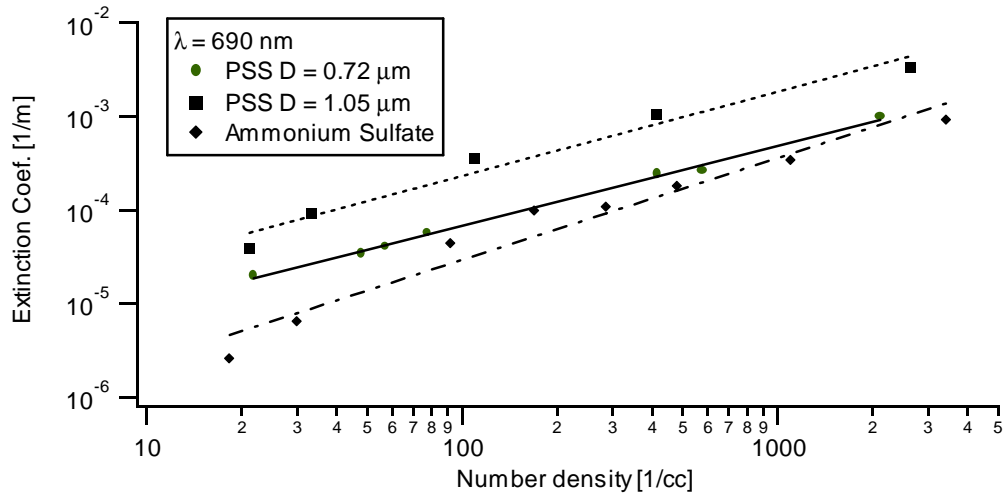


(b)

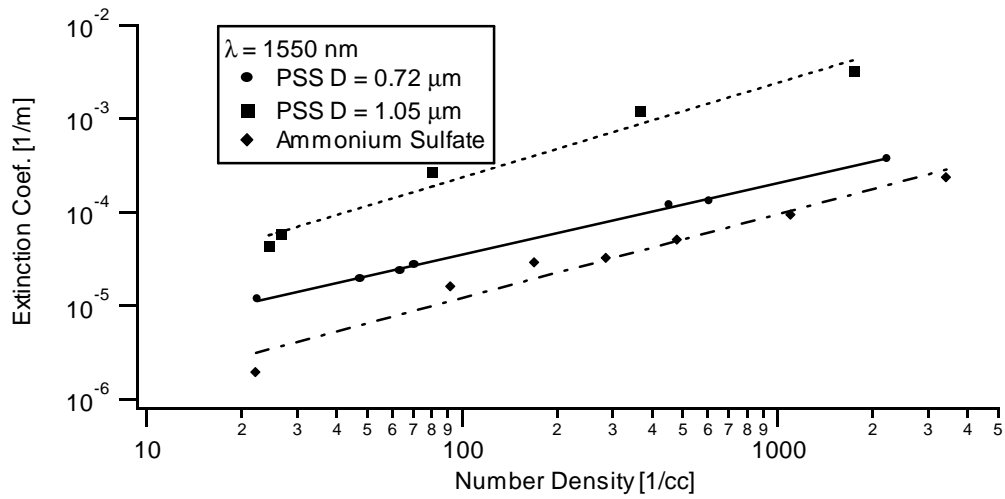


(c)

Figure 3. Comparison of Uncertainty for extinction and scattering coefficient and single-scattering albedo for various combinations of measurements.



(a)



(b)

Figure 4. Measurements of extinction coefficient versus number density for various aerosol composition and size. a) wavelength = 690 nm, b) wavelength = 1550 nm. (\reanal0108\idcomp)

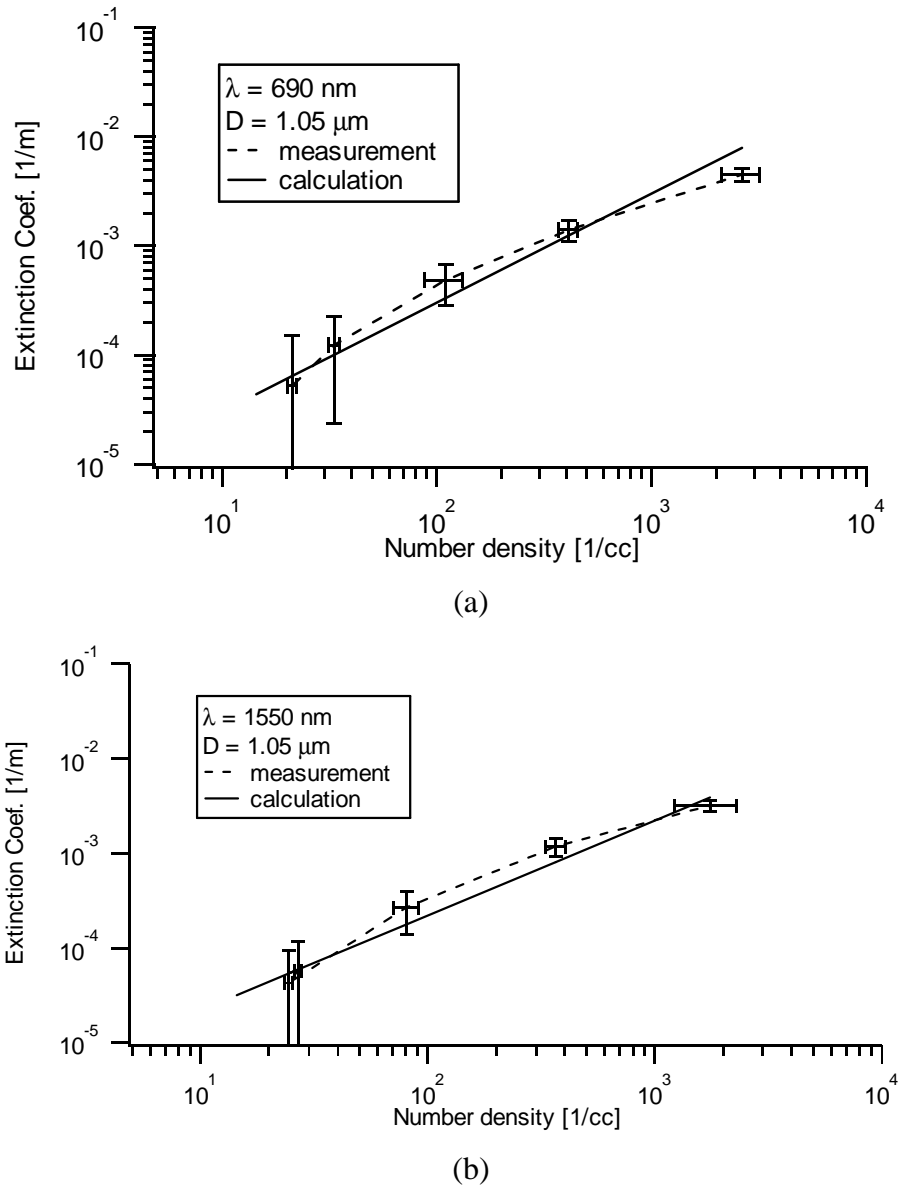


Figure 5. Measurements of extinction coefficient versus number density for 1.05 mm diameter polystyrene calibration spheres compared with Mie calculations. a) wavelength = 690 nm, b) wavelength = 1550 nm.

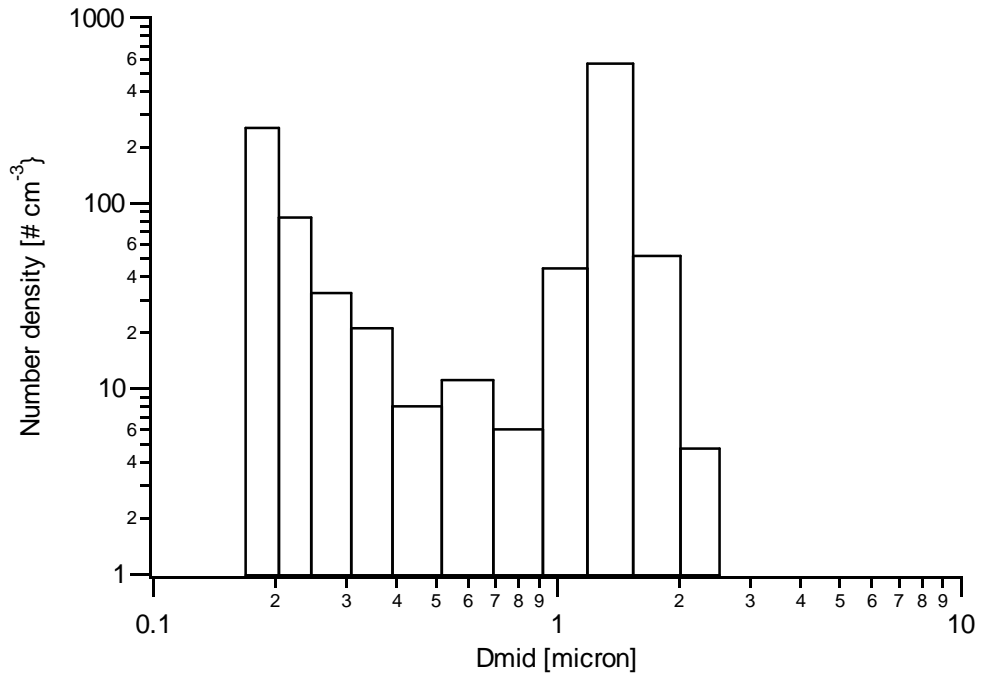
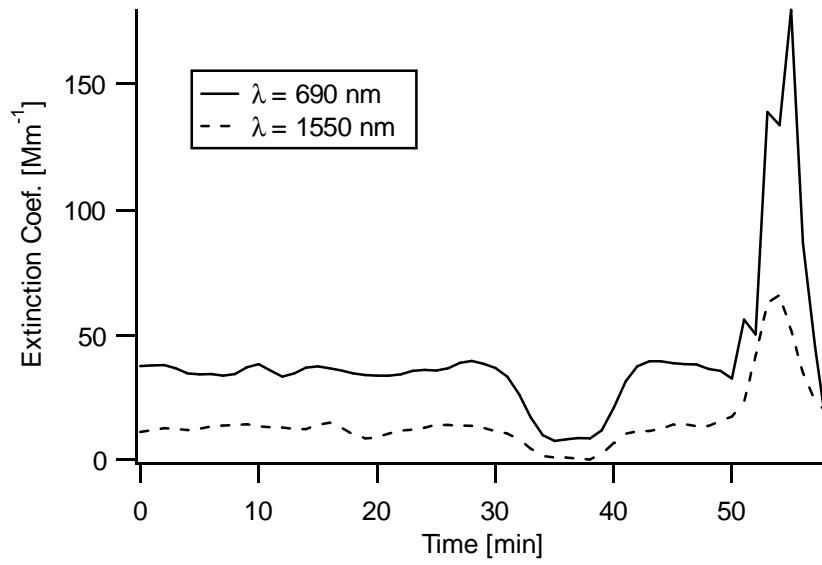
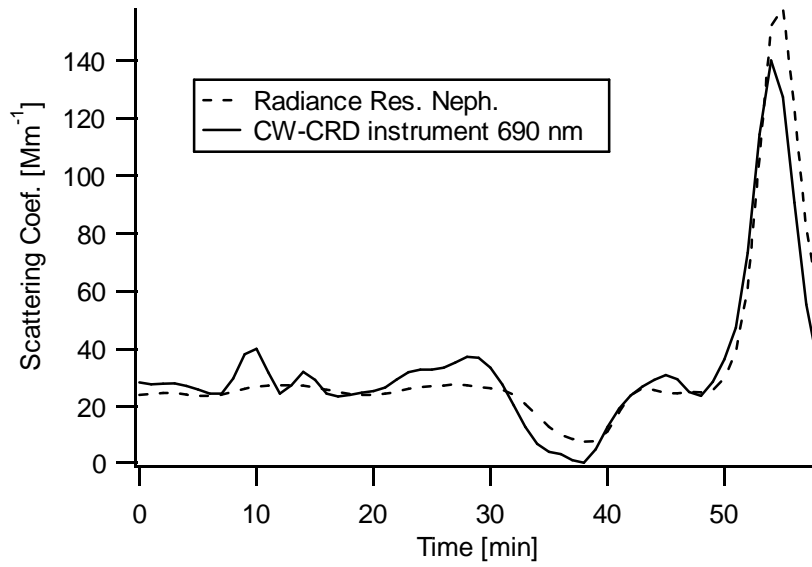


Figure 6. PCASP size distribution of 1.05 μm PSS with water. (pss1)



(a)



(b)

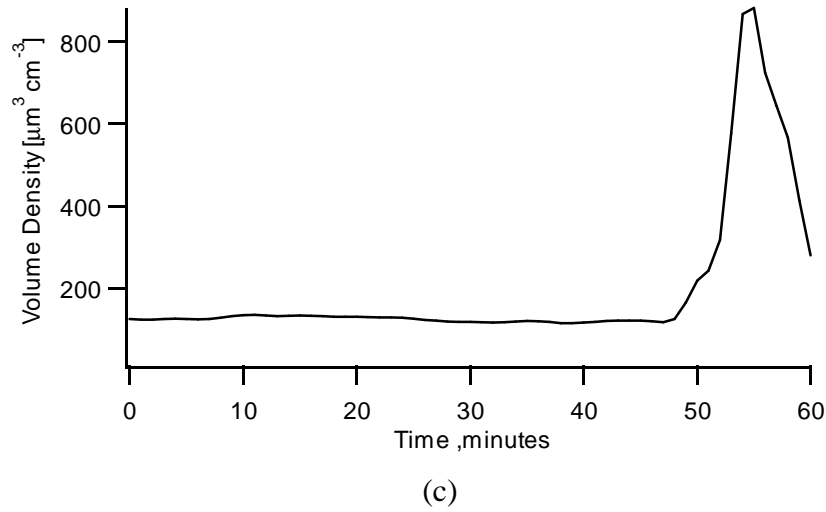


Figure 7. Field measurement. a) Extinction coefficient at both wavelengths; b) Prototype scattering measurement compared with Radiance Research nephelometer; c) volume density versus time from PCASP. The dip in signal in a and b at 35 minutes results from zero air. The peak at 50 minutes results from a plume encounter. renal_0108\r030303; pc030303

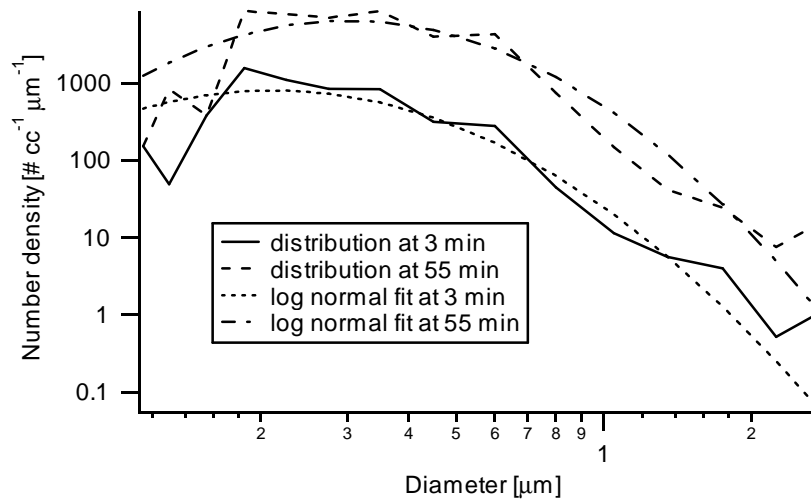


Figure 8. Size distributions from PCASP for two time periods, 3 and 55 minutes. Idtests_temp\pc030303